Two-pulse Width Modulation for Voltage Regulation and Reduction of Electromagnetic Field Radiated by Third Harmonic Current in Wireless Power Transfer System

1st Sakahisa Nagai
Department of Frontier Sciences
The University of Tokyo
Kashiwa, Japan
nagai-saka@edu.k.u-tokyo.ac.jp

2nd Toshiyuki Fujita
Department of Frontier Sciences
The University of Tokyo
Kashiwa, Japan

3rd Osamu Shimizu
Department of Frontier Sciences
The University of Tokyo
Kashiwa, Japan

4th Hiroshi Fujimoto
Department of Frontier Sciences
The University of Tokyo
Kashiwa, Japan

***Abstract*—Recently, wireless power transfer (WPT) for electric mobilities has much attention. The electromagnetic field radiated by the WPT current is limited by the international regulations. In order to reduce the electromagnetic field radiated by the third harmonic current (3rd-EMF) in an SS topology WPT system, the inverter is often operated using a phase shift control whose shifted phase is fixed at $\pi/3$ rad. However, an additional DC-DC converter is needed to control the WPT power. This paper proposes the two-pulse width modulation method to achieve both the voltage regulation and the 3rd-EMF reduction. The switching timing is determined by calculating Fourier transform of the inverter output voltage waveform. The proposed method is experimentally validated using a GaN inverter. The results show that the proposed method can regulate the voltage and reduce the third harmonic current simultaneously. The inverter efficiency is more than 92% when the duty ratio is more than 50% even if hard switching is conducted.**

***Index Terms*—wireless power transfer, pulse width modulation, harmonic electromagnetic field reduction**

I. Introduction

Recently, inductive wireless power transfer (WPT) techniques are developed for electric mobilities, such as electric vehicles (EVs), drones, railway vehicles, and so on [1]–[7]. The static WPT system is a user-friendly technology because the power is automatically charged when a mobility is parked on a charging pad [1], [2]. The dynamic WPT system is also studied to extend the cruising range and reduce the charging time and capacity of the battery, especially for EVs and drones [3]–[5]. In [7], a hybrid inductive and capacitive WPT system for autonomous mobilities was proposed to improve the power transfer, efficiency, and misalignment tolerance.

A WPT system radiates the electromagnetic field which may damage other electric devices and humans. To prevent the damages, international standard limits the electromagnetic field emission. Fig. 1 shows the magnetic radiation disturbance limit regulated in the international standard CISPR11 [8] and Japanese Radio Act [9]. Note that the limit level is different because the measurement distance from the equipment is different. In the case of the WPT for EVs, the fundamental frequency range from 79 to 90 kHz is used. The gray areas indicate the third, fifth, and seventh harmonic frequency ranges. As can be seen from the figure, the magnetic field disturbance of the low order harmonics needs to be suppressed.

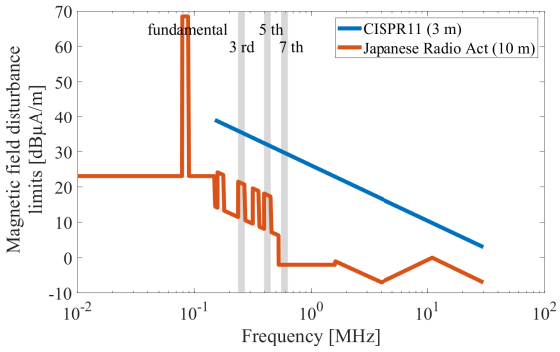

Fig. 1: Magnetic radiation disturbance limit.

This paper focuses on the reduction of the electromagnetic field radiated by the third harmonic current (3rd-EMF) in EV WPT system. The third-order harmonic component is the most severe against the limit shown in Fig. 1 because the higher harmonics can be suppressed by the band-pass characteristic of the resonant WPT circuit. The EMF reduction methods can be mainly divided into two methods: multiple-coil method [10]–[12] and inverter switching method [13]–[15]. The former method uses the cancellation of the magnetic field generated by the multiple coils. In [10], six coils

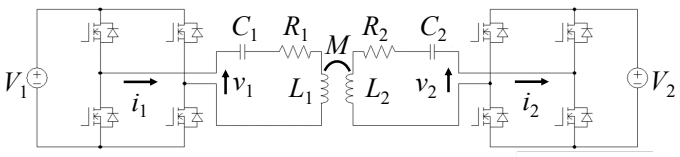

Fig. 2: SS circuit topology.

are used in both the transmitter and receiver sides and the transmitter coils are operated by three-phase inverter. In [11], a shielding coil is put on a transmitter coil and induced current flowing through the shielding coil reduces the leakage magnetic field. The multiple-coil method can suppress the magnetic field generated by not only the harmonics but also the fundamental component, however, the system becomes bigger compared with the other method. The later method uses the inverter switching to eliminate the specific order harmonic voltage (most cases are the third order). In the inverter typical operation, the output waveform becomes a square wave that includes odd harmonics. By using a phase shift control whose shifted phase is fixed at $\pi/3$ rad, the third harmonic component can be eliminated [13], [14]. In [15], multiple switching is conducted in the transmitter side to suppress not only the third harmonic component but also the other harmonic components. The inverter switching method is not required additional equipment such as coils and filters. However, the conventional switching methods cannot control the power because the switching phases are fixed. In order to control the power, an additional DC-DC converter is needed to change the inverter input voltage.

This paper proposes two-pulse width modulation to regulate the fundamental voltage for the power control and reduce the electromagnetic field radiated by the third harmonic current. The inverter output two pulses in a half period whose third harmonic voltage is always zero. The pulse width is changed to regulate the fundamental voltage. The effectiveness of the proposed method is experimentally confirmed using a GaN inverter.

This paper is organized as follows: Section II explains the SS circuit topology for the WPT. Section III explains the proposed two-pulse width modulation. The experimental results are shown in Section IV. Section V describes the conclusions of this paper.

II. SS CIRCUIT TOPOLOGY

This section describes the SS circuit topology for the WPT. The circuit diagram is shown in Fig. 2. V, I, v, and i are DC voltage, current, and high-frequency AC voltage and current, respectively. L, M, C, and R are self inductance, mutual inductance, capacitance, and resistance, respectively. The subscripts 1 and 2 mean the transmitter side and receiver side, respectively. The circuit equation can be written as

$$\begin{bmatrix} v_1 \\ v_2 \end{bmatrix} = \begin{bmatrix} Z_1 & -j\omega M \\ j\omega M & -Z_2 \end{bmatrix} \begin{bmatrix} i_1 \\ i_2 \end{bmatrix} \tag{1}$$

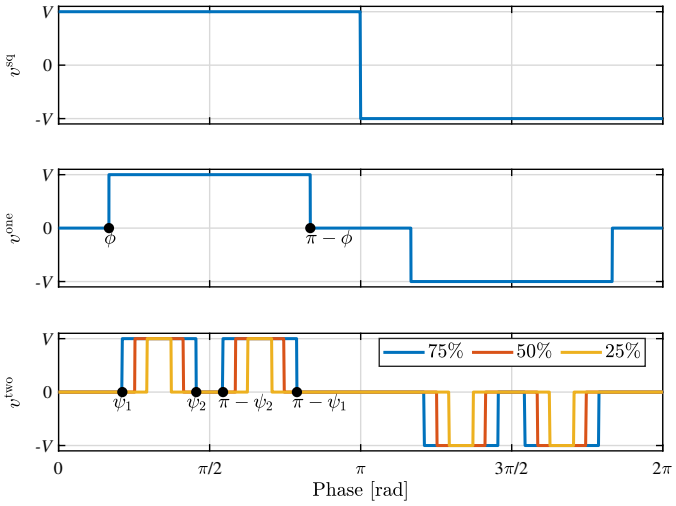

Fig. 3: Output voltage waveform of inverter.

where

$$Z_i = R_i + j\omega L_i + \frac{1}{j\omega C_i}. \tag{2}$$

ω is the resonant angular frequency which is calculated as

$$\omega = \frac{1}{\sqrt{L_i C_i}}. \tag{3}$$

When a load resistance R_{L} is connected to the output of the rectifier, the transmitter current and receiver coil current are calculated as

$$i_1 = \frac{R_2 + R_{\mathrm{L}}}{R_1 (R_2 + R_{\mathrm{L}}) + \omega^2 M} v_1. \tag{4}$$

$$i_2 = \frac{j\omega M}{R_1 (R_2 + R_{\mathrm{L}}) + \omega^2 M} v_1. \tag{5}$$

This paper focuses on the inverter output voltage regulation and the 3rd-EMF by the inverter switching. From (4) and (5), the reduction of the harmonics in v_1 decreases the harmonics in the current i_1 and i_2 and their generated electromagnetic field.

III. PROPOSED TWO-PULSE WIDTH MODULATION

This section describes the proposed two-pulse width modulation that can achieve the voltage regulation and 3rd-EMF reduction. The 3rd-EMF can be reduced by the inverter output voltage control to eliminate the third order harmonics. Fig. 3 shows the inverter output voltage, while the top figure indicates the waveform of the typical inverter operation v^{sq}, the center figure indicates the waveform of the 3rd-EMF with one-pulse width modulation v^{one}, and the bottom figure indicates the waveform of the proposed modulation v^{two} with the change of the duty ratio. The $(2k-1)$-th order harmonic component in each of the voltage waveforms is calculated by using Fourier transform as

$$v^{\mathrm{sq}}_{2k-1} = \frac{4V}{(2k-1)\pi} \tag{6}$$

$$v^{\mathrm{one}}_{2k-1} = \frac{4V}{(2k-1)\pi} \cos(2k-1)\phi \tag{7}$$

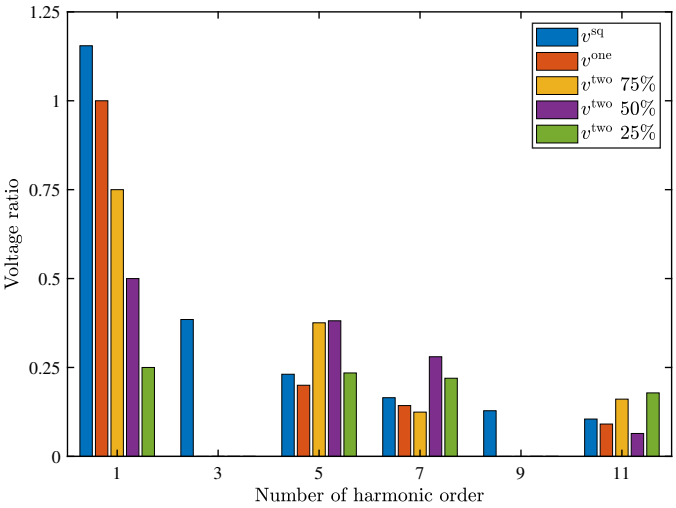

Fig. 4: Calculated harmonics in inverter output voltage waveform.

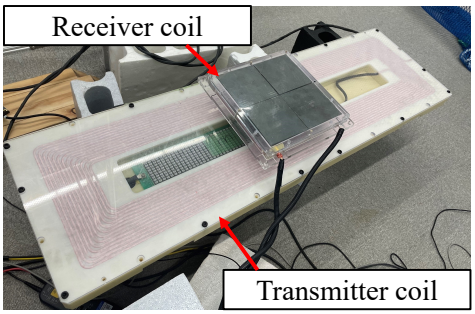

Fig. 5: Photograph of wireless power transfer coils.

$$v_{2k-1}^{\mathrm{two}} = \frac{4V}{(2k-1)\pi}\{\cos(2k-1)\psi_1 - \cos(2k-1)\psi_2\} \quad (8)$$

where k is a natural number. As shown in (6), the odd harmonics are included in the inverter output voltage. On the other hand, by setting ϕ at $\frac{\pi}{6}$ in (7), the third harmonic voltage is eliminated by one-pulse width modulation. However, the fundamental component becomes a constant of $\frac{2\sqrt{3}}{\pi}V$. In order to control the WPT power, an additional DC-DC converter must be connected before the inverter to change the inverter input voltage V.

In the proposed method, the fundamental component can be control with eliminating the third harmonic voltage. The phases ψ_1 and ψ_2 are the solutions of the following equations:

$$\begin{cases} v_1^{\mathrm{two}} = \frac{4V}{\pi}(\cos\psi_1 - \cos\psi_2) = v^{\mathrm{ref}} \\ v_3^{\mathrm{two}} = \frac{4V}{3\pi}(\cos 3\psi_1 - \cos 3\psi_2) = 0 \end{cases} \quad (9)$$

where v^{ref} is the reference voltage. The solutions are

$$\psi_1 = \arccos\frac{\tilde{v} + \sqrt{1 - \frac{\tilde{v}^2}{3}}}{2} \quad (10)$$

$$\psi_2 = \arccos\frac{-\tilde{v} + \sqrt{1 - \frac{\tilde{v}^2}{3}}}{2} \quad (11)$$

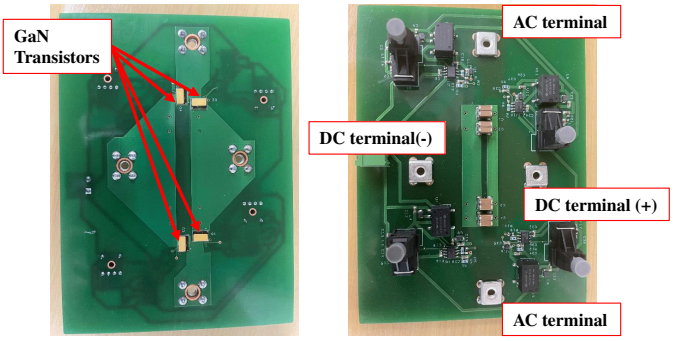

<Back side> <Front side>

Fig. 6: Photograph of GaN inverter (without a heat sink).

where

$$\tilde{v} = \frac{\pi v^{\mathrm{ref}}}{4V}. \quad (12)$$

The fundamental component can be controlled in the range of $0 \le v^{\mathrm{ref}} \le \frac{2\sqrt{3}}{\pi}V$. The legend of v^{two} in Fig. 3 is the duty ratio against the fundamental component of the one-pulse width modulation v^{one}. When the duty ratio is 100%, the voltage waveform becomes the same as the one-pulse width modulation v^{one}.

Fig. 4 shows the calculated result of the harmonics in the inverter output voltage. The vertical axis shows the voltage ratio against the fundamental component of the one-pulse width modulation v_1^{one}. The one-pulse width modulation and two-pulse width modulation can ideally eliminate the $3k$-th order harmonics. In addition, the proposed modulation can control the fundamental voltage at the reference duty ratio.

IV. Experiments

This section describes the experimental results. Fig. 5 shows photograph of the transmitter and receiver coils. The coils developed for the dynamic WPT for EVs [4] are used in the experiment. A vertical rectangular transmitter coil and square receiver coil are used. The experimental parameters are listed in Table I. The experiments were conducted with small power of about 600 W. In the experiments, a full-bridge diode rectifier is used in the receiver side. An electronic resistant load whose load value is fixed is used despite the voltage source in the receiver side. In order to generate the voltage waveform, a GaN inverter shown in Fig. 6 is used in the transmitter side. GaN power transistors "GS66508B" produced by GaN Systems is utilized in the inverter. A heat sink is attached on the back side when the WPT experiment is conducted. The gate signals are generated using an FPGA controller whose clock frequency is 200 MHz.

Figs. 7-11 shows the experimental waveforms of the typical inverter operation, one-pulse width modulation, two-pulse width modulation with change of duty ratio at 75%, 50%, and 25%, respectively. Each figure includes the waveforms of the inverter output voltage v_1, transmitter current i_1, rectifier input voltage v_2, and receiver current i_2. From the inverter output voltage waveform, it is confirmed that the inverter

TABLE I: Parameters.

Self inductance	L_1, L_2	245.9, 105.4 μH
Mutual inductance	M	24.23 μH
Capacitance	C_1, C_2	13.6, 31.8 nF
Resistance	R_1, R_2	401, 104 mΩ
Operating frequency	$\omega/2\pi$	87 kHz
Dead time		40 ns
DC voltage	V_1	100 V
Load resistance	R_L	12.5 Ω
FPGA clock frequency		200 MHz

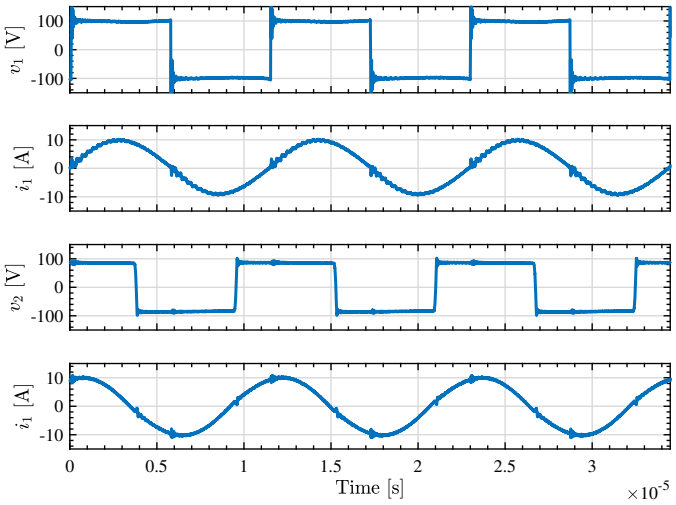

Fig. 7: Experimental waveforms. (Typical inverter operation.)

properly generate the waveform as shown in Fig. 3. The transmitter current is reduced when the duty ratio decreases. The transmitter current i_1 is calculated as shown in (4). Therefore, i_1 is proportional to v_1. By regulating v_1 by the proposed method, i_1 can be changed. At the moment of the inverter switching, the waveforms of i_1 and i_2 are slightly oscillated. This is the measurement noise caused by the fast switching of the GaN.

Fig. 12 shows the calculated harmonics in the inverter output voltage v_1 and transmitter current i_1. The vertical axes show the voltage ratio and current ratio against the fundamental component of the one-pulse width modulation. From Fig. 12(a), it is confirmed that the results are similar to the calculated results in Fig. 4. The fundamental component of the two-pulse width modulation should be the same with the reference duty, however, the calculated value is slightly small. The reason is that the dead time reduces the pulse width. As for a future work, the dead time compensation will be implemented to achieve more accurate voltage regulation. In addition, the third and even harmonic components theoretically become zero as shown in Fig. 4, however, they could not be eliminated as shown in Fig. 12(c). The main reason is the ringing by the hard switching.

From Fig. 12(b), it is confirmed that the third harmonic current greatly suppressed by the proposed method. On the other hand, the fifth-order harmonic component got worse because the two-pulse width modulation could only eliminate the third-order harmonics. As a future work, the two-pulse

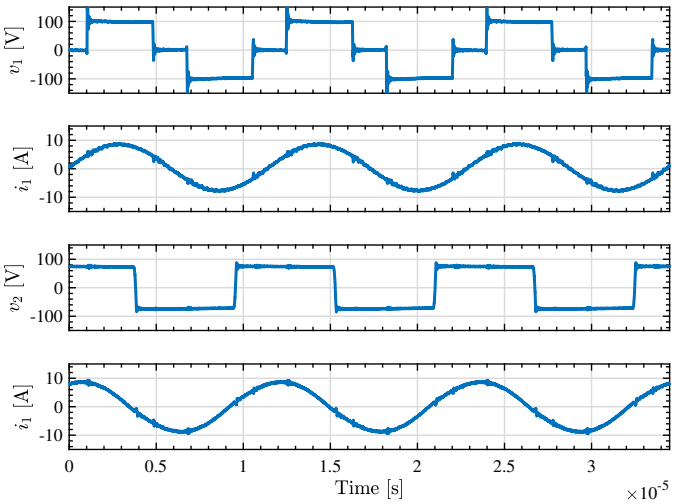

Fig. 8: Experimental waveforms. (One-pulse width modulation.)

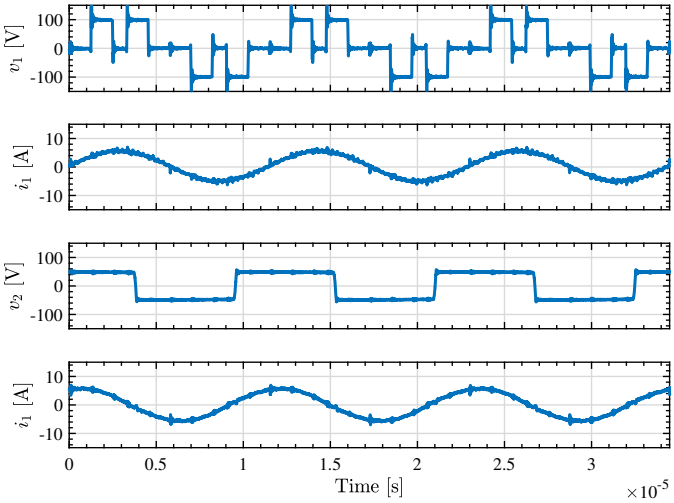

Fig. 9: Experimental waveforms. (Two-pulse width modulation with duty 75%.)

width modulation with low total harmonic distortion will be discussed.

Finally, Table II shows the comparison of the power and efficiency. The power and efficiency are measured using a power analyzer "PW6001" produced by HIOKI E. E. CORPORATION. The experiments were conducted using a constant load, therefore, the transferred power should be inverse proportional to the square of the duty ratio. The input power was less than the value calculated from the duty ratio because of the dead time and diode rectifier efficiency. The dead time reduces the fundamental component of the inverter output voltage as shown in Fig. 12(a). In the receiver side, the DC voltage is reduced because the receiver current is reduced by the voltage regulation. The diode forward voltage affect the rectifier efficiency as shown in Table II when the transferred power decreases.

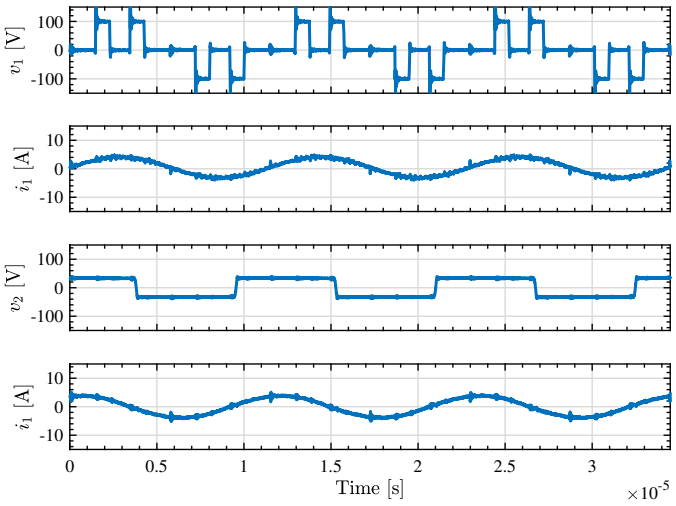

Fig. 10: Experimental waveforms. (Two-pulse width modulation with duty 50%.)

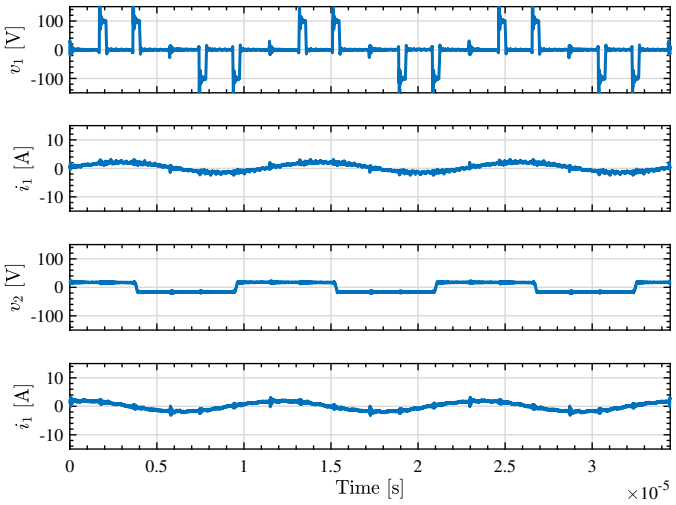

Fig. 11: Experimental waveforms. (Two-pulse width modulation with duty 25%.)

From the efficiency results, the inverter efficiency decreases when the duty ratio decreases. The proposed method must be done the hard switching as shown in Figs. 9-11. However, thanks to the GaN fast switching, the inverter efficiency is more than 92% when the duty ratio is more than 50%.

V. Conclusions

This paper proposes the pulse width modulation method which can achieve both the inverter output voltage regulation and the 3rd-EMF reduction in WPT system. The inverter output two pulses during the half period. The third harmonic voltage becomes always zero and the pulse width can regulate the fundamental voltage. Experiments were carried out to validate the proposed method. A GaN inverter is utilized to realize the fast switching. The experimental results show that the fundamental component can be regulated by changing the duty ratio with the reduction of the 3rd-EMF. In addition, the power and efficiency are experimentally compared. As a result,

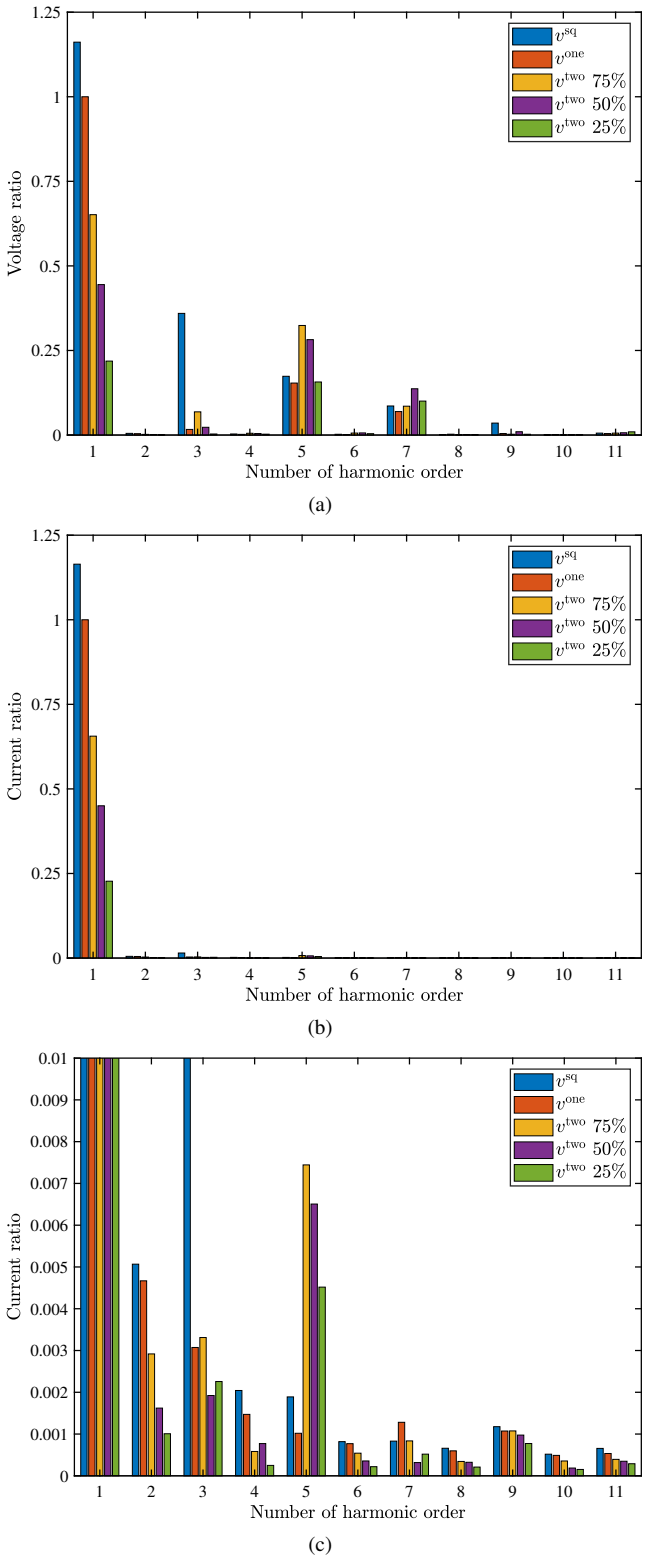

Fig. 12: Calculated harmonics. (a) Inverter output voltage v_1. (b) Transmitter current i_1. (c) Transmitter current i_1 (enlarged: 0–0.01 current ratio).

TABLE II: Comparison of power and efficiency.

	Typical	One-pulse	Two-pulse (75%)	Two-pulse (50%)	Two-pulse (25%)
DC input power [W]	603	444	193	91.8	25.3
DC output power [W]	563	413	174	80.4	18.9
Inverter efficiency [%]	97.64	97.68	95.27	92.20	77.11
Rectifier efficiency [%]	98.57	98.34	97.40	96.26	92.76
DC-to-DC efficiency [%]	93.48	93.2	90.39	87.53	74.64

the total DC-to-DC efficiency decreased with the decrease of the duty ration because of the hard switching of the inverter and decrease of the diode rectifier efficiency. However, when the duty ratio is more than 50%, the inverter efficiency of 92% is achieved. As for future works, the dead time compensation will be done to output the voltage more precisely, and the WPT power control with a feedback control will be done. This proposal is useful for a lot of applications because the voltage regulation and the 3rd-EMF reduction can be done without additional DC-DC converter before the inverter.

ACKNOWLEDGMENT

This work was partly supported by JSPS KAKENHI Grant Number JP22K14234, the New Energy and Industrial Technology Development Organization (NEDO) Project Number JPNP21005, JPNP21014, and JST-Mirai Program Grant Number JPMJMI21E2, Japan.

REFERENCES

[1] M. M. Ahmed, M. A. Enany, A. A. Shaier, H. M. Bawayan, and S. A. Hussien, "An Extensive Overview of Inductive Charging Technologies for Stationary and In-Motion Electric Vehicles," *IEEE Access*, Vol. 12, pp. 69875–69894, 2024.

[2] X. Wang, M. Leng, X. Zhang, Q. Tian, X. Zhou, B. Guo, and H. Ma, "Multioutput Wireless Charger for Drone Swarms With Reduced Switch Requirements and Independent Regulation Capability," *IEEE Transactions on Industrial Electronics*, Vol. 71, No. 5, pp. 4883–4895, 2024.

[3] V. Z. Barsari, D. J. Thrimawithana, S. Kim, and G. A. Covic, "Modular Coupler With Integrated Planar Transformer for Wireless EV Charging," *IEEE Trans. Power Electronics*, Vol. 38, No. 7, pp. 9206–9217, 2023.

[4] O. Shimizu, T. Fujita, S. Nagai, H. Fujimoto, and Y. Omori, "Development of Dynamic Wireless Power Transfer Coils for 3rd Generation Wireless In-wheel Motor", *Electrical Engineering in Japan*, Vol. 214, No. 4, pp. 638–645, 2021.

[5] K. Chen and Z. Zhang, "In-Flight Wireless Charging: A Promising Application-Oriented Charging Technique for Drones," *IEEE Industrial Electronics Magazine*, Vol. 18, No. 1, pp. 6–16, 2023.

[6] E. Sato and K. Kondo, "Feasible Power Control Method with a Low Sampling Frequency for Bidirectional Wireless Power Transfer in Battery-Powered Railway Vehicle Systems", *IEEJ Journal of Industry Applications*, Vol. 12, No. 6, pp. 1078–1087, 2023.

[7] D. Vincent, P. S. Huynh, and S. S. Williamson, "A Link-Independent Hybrid Inductive and Capacitive Wireless Power Transfer System for Autonomous Mobility," *IEEE Journal of Emerging and Selected Topics in Industrial Electronics*, Vol. 3, No. 2, pp. 211–218, 2022.

[8] International Electrotechnical Commission, "Industrial, Scientific and Medical Equipment - Radio-Frequency Disturbance Characteristics - Limits and Methods of Measurement CISPR11," Ed. 7.0, 2024.

[9] Ministry of Internal Affairs and Communications, Radio Act, Act No. 131, https://www.japaneselawtranslation.go.jp/en/laws/view/3205 (Japanese Law Translation)

[10] K. Kusaka, K. Furukawa, and J. Itoh, "Development of Three-Phase Wireless Power Transfer System with Reduced Radiation Noise", *IEEJ Journal of Industry Applications*, Vol. 8, No. 4, pp. 600–607, 2019.

[11] C. Lee, S. Woo, Y. Shin, J. Rhee, and S. Ahn, "Reactive Shielding Method for Wireless Power Transfer Systems with High Power Transfer Efficiency using Frequency Split Phenomena," in *Proc. of 2023 IEEE Symposium on Electromagnetic Compatibility & Signal/Power Integrity (EMC+SIPI)*, pp. 560–565, 2023.

[12] K. Kusaka, K. Yamagata, J. Katsuya, and T. Sato, "Reduction in Leakage Magnetic Flux of Wireless Power Transfer Systems with Halbach Coils," *IEEJ Journal of Industry Applications*, Vol. 12, No. 6, pp. 1104–1105, 2023.

[13] H. Kim, S. Jeong, D.-H. Kim, J. Kim, Y.-I. Kim and I.-M. Kim, "Selective Harmonic Elimination Method of Radiation Noise from Automotive Wireless Power Transfer System Using Active Rectifier," *2016 IEEE 25th Conference on Electrical Performance Of Electronic Packaging And Systems (EPEPS)*, pp. 161–164, 2016.

[14] T. Yanagi, K. Nakahara, H. Sumiya, S. Nagai, O. Shimizu and H. Fujimoto, "Effect of the Conduction Resistance of SiC MOSFET on the Harmonics of Inverter Voltage in Wireless Power-Transfer Systems for Electric Vehicles," *IEEE Access*, Vol. 12, pp. 86886–86895, 2024.

[15] D. Kobuchi, K. Matsuura, Y. Narusue, and H. Morikawa, "Cancellation of Harmonics in the Magnetic Field Leakage from Inductive Power Transfer Systems," *IEEE Trans. Vehicular Technology*, Vol. 72, No. 4, pp. 4442–4452, 2025.